Path Integral Computation of Lowest Order Modes in Arbitrary-Shaped Inhomogeneous Waveguides

Vincenzo Galdi, Vincenzo Pierro, and Innocenzo M. Pinto

***Abstract*— A general numerical algorithm for the computation of the fundamental modes and related cutoff wavenumbers in arbitrary shaped inhomogeneous waveguides is presented. The method exploits a generalized Donsker-Kač formula to express the lowest order modes in terms of asymptotic generalized Wiener-Itô integrals, whose computation is carried out by means of Monte Carlo methods. Comparison with known solutions and computational budget indicate that the proposed method is indeed accurate, versatile, as well as computationally efficient.**

***Index Terms*— Guided waves, Monte Carlo methods, path integrals.**

I. Introduction

IN THIS LETTER we try to give a hopefully comprehensive description of a new method for the computation of the dominant modes in z-uniform inhomogeneous waveguides having arbitrary transverse shape. The algorithm is based upon Donsker-Kač formula [1], well known in quantum mechanics, but not yet properly exploited, if not at all, in electromagnetics. Recently we proposed the use of this formula to compute the fundamental mode in complex dielectric structures [2]. Subsequently we succeeded in extending the formula to allow the treatment of Dirichlet or Neumann boundary conditions, typical of metallic waveguides.

II. Generalized Donsker-Kač Formula

An n-dimensional second-order differential operator is considered on a compact subset $\mathcal{D} \subseteq R^n$ with regular boundary $\partial\mathcal{D}$,

$$L = \frac{1}{2}\sum_{i,j=1}^{n} b^{ij}\frac{\partial^2}{\partial x^i \partial x^j} + \sum_{i=1}^{n} a^i \frac{\partial}{\partial x^i}. \tag{1}$$

The associated scalar Helmholtz eigenvalue problem with homogeneous Dirichlet or Neumann boundary conditions:

$$\begin{aligned} L\phi(\underline{x}) - [V(\underline{x}) - \lambda]\phi(\underline{x}) &= 0, \qquad \underline{x} \in \mathcal{D}, \\ \phi(\underline{x}) = 0 \quad \text{or} \quad \frac{\partial\phi}{\partial n}(\underline{x}) &= 0, \qquad \underline{x} \in \partial\mathcal{D} \end{aligned} \tag{2}$$

V being a regular real function, has a discrete spectrum of real eigenvalues [3], $\lambda_1 < \lambda_2 < \lambda_3 < \cdots$, and associated eigenfunctions $\phi_j, j = 1, 2, 3, \cdots$ forming an orthonormal system in $L^2(\mathcal{D})$ [4].

Manuscript received July 23, 1997.

The authors are with the Dipartimento di Ingegneria dell'Informazione e Ingegneria Elettrica, University of Salerno, Salerno, Italy.

Publisher Item Identifier S 1051-8207(97)08979-4.

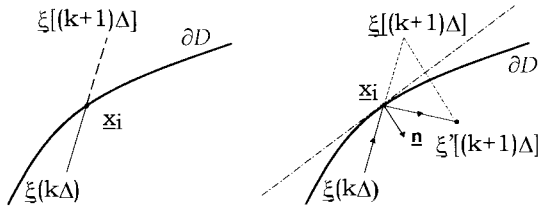

Fig. 1. Enforcing boundary conditions on the Itô process. (a) Dirichlet boundary conditions: path ends at $\underline{x}_i$ (absorbing). (b) Neumann boundary conditions: path is specularly reflected, $\underline{\xi}[(k+1)\Delta]\} \rightarrow \underline{\xi}'[(k+1)\Delta]\}$.

The Donsker-Kač formula [1], used for computing the lowest eigenvalue (eigenfunction) of the problem (2) with $\mathcal{D} = R^n$ and regularity-at-infinity conditions (dielectric waveguides [2]), can be generalized to *bounded* domains and Dirichlet or Neumann boundary conditions, yielding

$$\lambda_1 \sim \frac{\log\left\{\dfrac{E_{\underline{x}}\left[f[\underline{\xi}(T_1)]\exp\left\{-\displaystyle\int_0^{T_1} V[\underline{\xi}(s)]\,ds\right\}\right]}{E_{\underline{x}}\left[f[\underline{\xi}(T_2)]\exp\left\{-\displaystyle\int_0^{T_2} V[\underline{\xi}(s)]\,ds\right\}\right]}\right\}}{T_2 - T_1} \tag{3}$$

$$\phi_1(\underline{x}) \sim C E_{\underline{x}}\left[f[\underline{\xi}(T)]\exp\left\{-\int_0^{T} V[\underline{\xi}(s)]\,ds\right\}\right] \tag{4}$$

where $T_2 > T_1, C$ is a normalization constant and the equality holds for $T, T_1, T_2 \longrightarrow \infty$. The symbol $E_{\underline{x}}$ represents a functional integral (expectation value [5]), on the probability measure associated to the Itô process $\underline{\xi}(s)$ of initial point $\underline{x}$, generated [8] by the operator L under path *absorption* (Dirichlet boundary conditions) or path *reflection* (Neumann boundary conditions) at the boundary $\partial\mathcal{D}$ (see Fig. 1) [6], [7], and f is a suitable *weight* function.[1] The Itô process $\underline{\xi} = (\xi^1, \cdots, \xi^n)$, in the domain $\mathcal{D}$ is ruled by the following stochastic integral equation [6], [8]:

$$\xi^i(s) = x^i + \int_0^s a^i[\underline{\xi}(\tau)]\,d\tau + \sum_{j=1}^{n}\int_0^s \sqrt{b^{ij}[\underline{\xi}(\tau)]}\,dw_\tau^i \tag{5}$$

$\{dw_\tau^i\}_{i=1,\cdots,n}$ being independent one-dimensional Wiener differentials [8].

[1] The weight function must be not orthogonal to the principal eigenfunction, and for Dirichlet boundary conditions it must be zero at the boundary. The choice of a weight function with the same symmetry properties as the sought eigenfunction can highly improve the accuracy.

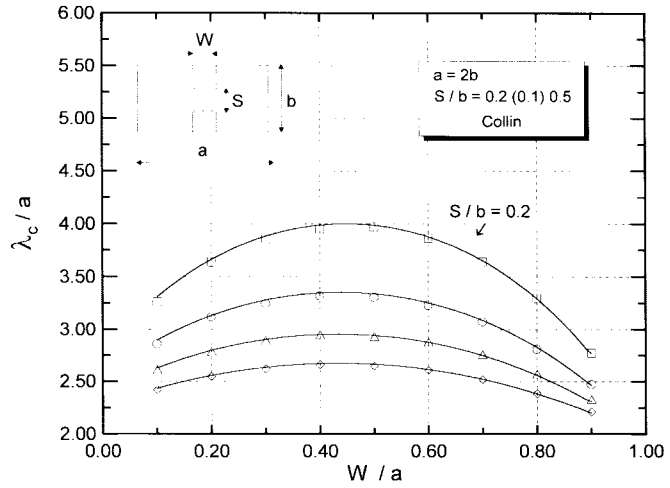

Fig. 2. Double-ridge waveguide. Scaled cutoff wavelength versus scaled ridge-width (TE fundamental mode) at various S/b values. Continuous line: std. solution ([11, p. 205]); markers: GDK method.

III. Numerical Implementation and Results

The needed functional integrals can be computed without any restriction on geometrical and/or constitutive complexity using Monte Carlo methods [9], [10]. For conciseness, here we limit ourselves to roughly outline the whole procedure adopted, skipping specific questions (e.g. the choice of parameters). More details may be found in [2]. The fundamental steps to compute the functional integral $E_{\underline{x}}\{g[\underline{\xi}(\cdot);T]\}$ in (3), (4) can be summarized as follows:

1) path generation: i.e., discrete-time (step-size Δ) approximation for the Itô process involved, in the interval $[0,T]$, with the suitable behavior at the boundary (see Fig. 1);
2) evaluation of the functional g on the path;
3) iteration of the procedure and evaluation of the first- and second-order moments $\mu_1(\Delta,M),\mu_2(\Delta,M)$, where M is the total number of paths.

The functional integral can be accordingly computed as a double limit:

$$E_{\underline{x}}\{g[\underline{\xi}(\cdot);T]\}=\lim_{\Delta\to 0}\lim_{M\to\infty}\mu_1(\Delta,M). \tag{6}$$

Obviously, for finite values of Δ,M the estimation will be affected by: 1) a systematic error, due to the effect of time-discretization, $\epsilon_{\rm sys}\sim\mathcal{O}(\Delta)$, and 2) a statistical error [9], [10], $\epsilon_{\rm stat}\sim\mathcal{O}(M^{-1/2})$. The confidence interval of the estimated functional integral is thus

$$\delta(M,\Delta)=\mu_1(M,\Delta)\pm\alpha M^{-1/2}[\mu_2(M,\Delta)-\mu_1^2(M,\Delta)]^{1/2} \tag{7}$$

where α depends of the sought confidence level. As a first example of application of the Generalized Donsker-Kač (henceforth GDK) method, we consider a homogeneous rectangular waveguide with a double (symmetrical) ridge. For such a structure no analytical solutions are known, but several approximations are available. One of the most popular approximations (see e.g., [11]) is based on the transverse resonance method and quasistatic conformal mapping. Fig. 2 shows the GDK computed normalized cutoff wavelength (as a function of the normalized ridge-width, at several values of the ridge spacing) compared with those obtained from the above approximation, for the fundamental (quasi-TE_{10}) mode. A very good agreement is observed. Fig. 3 shows the behavior of the corresponding eigenfunction.

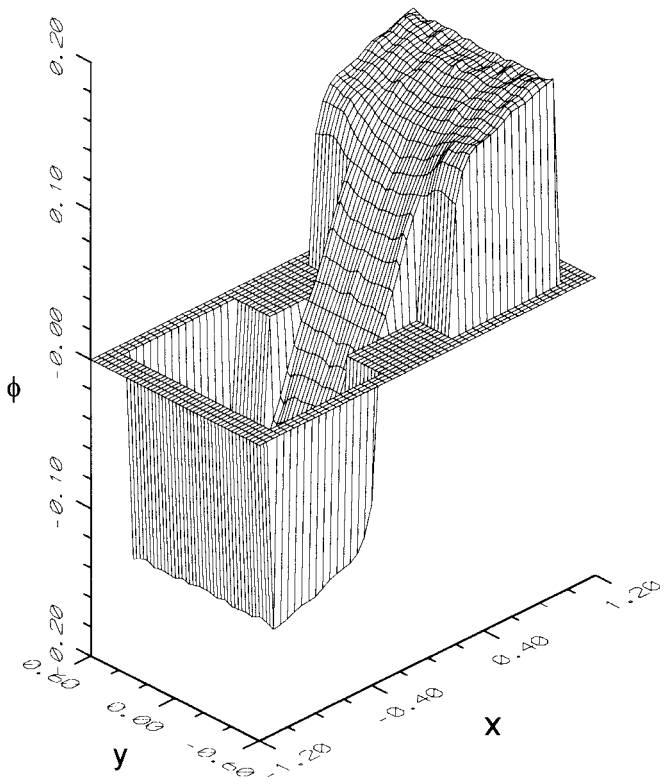

Fig. 3. Double-ridge waveguide. TE fundamental mode. ($a=2b=2$, $W/a=0.3, S/b=0.5$.)

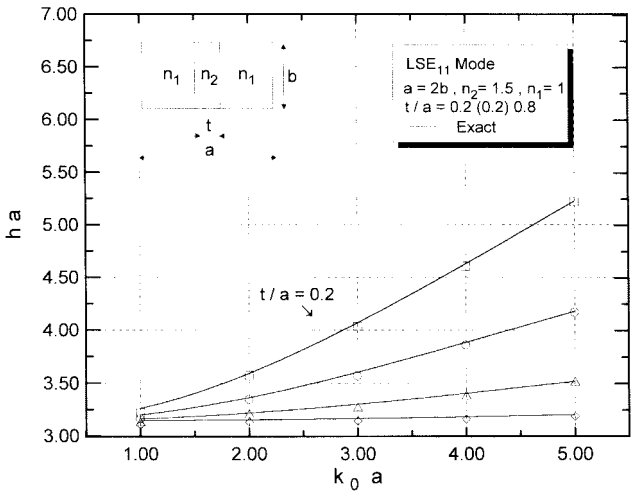

Fig. 4. Dielectric loaded rectangular waveguide. LSE_{11} mode dispersion diagram ($h=[k_0^2n_1^2-(\pi/b)^2]^{1/2}$) at various values of dielectric slab thickness. Continuous line: exact solution; markers: GDK method.

As a second example we consider a rectangular waveguide loaded with a dielectric slab (see Fig. 4). In this case analytical solutions are easily obtained by applying the transverse resonance technique [11]. In Fig. 4 we report the exact dispersion curves (scaled modal parameter versus scaled free-space

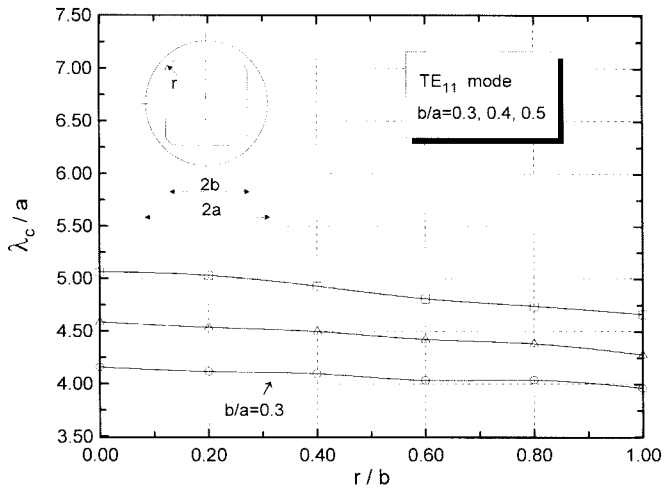

Fig. 5. Coaxial waveguide with rounded-corner-square inner conductor. Scaled cutoff wavelength of first TE mode versus scaled rounded-corner radius at various values of scaled square-width.

wavenumber), together with the GDK computed values for the fundamental LSE mode. Also in this case the observed agreement is very good.

Finally a rather odd structure is analyzed, namely a circular waveguide with a coaxial rounded-corner-square. Considerable interest has been shown for such a geometry in particle accelerators design (LHC project, [12]). In this connection, computation of the cutoff frequency of the first TE mode represents an important issue, related to beam stability. In Fig. 5 we report the normalized cutoff wavelength as a function of the rounded-corner radius, at several values of the square width.

In order to obtain all results above, a typical number $M \sim 10^5$ paths with an adaptive timestep ($\Delta \sim 10^{-5}$ close to the boundary, where the evolution of the path is more critical, $\Delta \sim 10^{-3}$ elsewhere) have been used. Values of T, T_1, T_2 in excess of $2\lambda_1^{-1}, \lambda_1$ being the estimated eigenvalue, ensure that the limit for $T, T_1, T_2 \to \infty$ implied in (3) and (4) is essentially achieved (see also [2]).

IV. Comparison with Usual Techniques

The main merits of the proposed method as compared to standard methods (e.g., finite elements methods [13], methods of moments [14]), can be summarized as follows:

- very easy implementation: no need for meshing algorithms and basis functions choice;
- very mild storage requirements;
- intrinsically *fully parallel*[2];
- computational burden growing *only* linearly with *both* problem size (characteristic-length/wavelength) *and* spatial embedding dimension n.

On the other hand, its main drawbacks are:

- lowest order modes, and scalar problems only;
- relatively slow convergency rate ($\propto M^{-1/2}$).

As a conclusion the presented method seems particularly suitable for the analysis of (the fundamental modes of) complex structures, whenever fast computing (possibly parallel) engines and relatively little memory are available.

References

[1] M. D. Donsker and M. Kač, "A sampling method for determining the lowest eigenvalue and the principal eigenfunction of Schrödinger equantion," *J. Res. NBS*, vol. 44, p. 551, 1950.
[2] V. Galdi, V. Pierro, and I. M. Pinto, "Cut-off frequency and dominant eigenfunction computation in complex dielectric geometries via Donsker-Kač formula and Monte Carlo method," *Electromagnetics*, vol. 17, no. 1, pp. 1–14, Jan. 1997.
[3] D. Ray, "On spectra of second-order differential operators," *Trans. Amer. Math. Soc.*, vol. 77, pp. 299–321, 1954.
[4] M. Reed and B. Simon, *Methods of Modern Mathematical Physics*, II. New York: Academic, 1975.
[5] I. M. Gelfand and A. M. Yaglom, "Integration in functional spaces and its applications in quantum physics," *J. Math. Phys.*, vol. 1, p. 48, 1960.
[6] I. I. Gihman and A. V. Skorohod, *Stochastic Differential Equations*. Berlin, Germany: Springer-Verlag, 1972.
[7] A. Gerardi, F. Marietti, and A. M. Rosa, "Simulation of diffusions with boundary conditions," *Syst. Contr. Lett.*, vol. 4, pp. 253–261, July 1984.
[8] C. W. Gardiner, *Handbook of Stochastic Methods for Physics, Chemistry and Natural Sciences*. Berlin, Germany: Springer-Verlag, 1983.
[9] I. M. Sobol, *The Monte Carlo Method*. Moscow. USSR: MIR, 1975.
[10] P. E. Kloeden and E. Platen, *Numerical Solution of Stochastic Differential Equations*. New York: Springer, 1991.
[11] R. E. Collin, *Foundations for Microwave Engineering*. New York: McGraw-Hill, 1992.
[12] The LHC study group, CERN/AC/95-05 (LHC), 1995.
[13] P. P. Silvester and R. L. Ferrari, *Finite Elements for Electrical Engineering*. Cambridge, U.K.: Univ. Press, 1990.
[14] R. F. Harrington, *Field Computation by Moment Methods*. New York: McMillan, 1968.

[2] All repeated operations (path generation, functional evaluation) can be performed independently and so can be easily and fully distributed among parallel processors.